NeuroImage 259 (2022) 119405

Contents lists available at ScienceDirect

NeuroImage

journal homepage: www.elsevier.com/locate/neuroimage

Similarity-based fMRI-MEG fusion reveals hierarchical organisation within the brain's semantic system

Elisa Leonardelli[a], Scott L. Fairhall[b,*]

[a] Fondazione Bruno Kessler, Trento, Italy
[b] Center for Mind/Brain Sciences, University of Trento, Italy

A B S T R A C T

Our ability to understand and interact with our environment relies upon conceptual knowledge of the meaning of objects. This process is supported by a distributed network of frontal, parietal, and temporal brain regions. Insight into the differential roles of various elements of this system can be inferred from the timing of activation, and here we use similarity-based fMRI-MEG fusion to understand when the representational spaces in different elements of the semantic system converge with representational spaces in the evolving MEG signal. Participants performed a semantic-typicality judgement of written words drawn from nine different semantic categories in separate fMRI and MEG sessions. Results indicate an initial period of congruence between MEG and fMRI informational spaces dominated by the posterior inferior temporal gyrus and the ventral temporal cortex between 350 and 450 msec. This is followed by a second period of convergence between 450 and 795 msec where MEG and fMRI representational spaces conform in left angular gyrus and precuneus in addition to ventral temporal cortex. Results are consistent with the multistage recruitment of the semantic system, initially involving automatic aspects of the representational system and later extending to broader elements of the semantic system more strongly associated with internalised cognition.

Conceptual representation allows us to understand the meaning of the objects we perceive and is critical for effective interaction with the environment and provides many of the necessary building blocks for higher thought. Functional magnetic resonance imaging (fMRI) research has identified a distributed network of brain regions that reliably activate more strongly to semantically richer stimuli (e.g. words versus pseudowords) or semantically engaging tasks (e.g. semantic versus phonological decision tasks; Binder et al., 2009). This general semantic processing of word stimuli recruits a left-lateralised cortical network encompassing several heteromodal associative regions (the angular gyrus (AG), lateral temporal cortex, ventral temporal cortex, dorsomedial and ventromedial prefrontal cortex (dm/vmPFC), inferior frontal gyrus (IFG), and the precuneus; Binder et al., 2009).

This network incorporates regions thought to guide and control semantic access: the lateral PFC, dmPFC and potentially the posterior middle temporal gyrus (pMTG; Badre et al., 2005; Jackson, 2021; Lambon-Ralph et al., 2017; Martin and Chao, 2001; Thompson-Schill et al., 1997; Wagner et al., 2001; Whitney et al., 2011). Other components of the semantic system fall within the default mode network (DMN; Binder et al., 2009), a network of functionally coupled regions generally more active during rest periods and deactivated during cognition that requires cognitive control (Buckner et al., 2008). These regions are candidate components of the representational system and include the precuneus, the AG, lateral MTG and anterior aspects of the ventral temporal cortex. In addition to showing a stronger univariate response to semantically richer stimuli, these brain areas exhibit multivariate sensitivity to the semantic content of single words (Bruffaerts et al., 2013; Devereux et al., 2013; S.L. S.L. Fairhall and Caramazza, 2013; Liuzzi et al., 2020, 2015; Simanova et al., 2014). These regions may work in tandem with neural populations outside this network that encode sensory- and modality-relevant information (Lambon-Ralph et al., 2017; Patterson et al., 2007; Tyler and Moss, 2001), and multiple regions within the brain show selective variation in response amplitude during semantic access to different categories of knowledge (e.g. motor-, tool-, person- or place-related knowledge; Fairhall, 2020; Fairhall et al., 2014; S.L. Fairhall and Caramazza, 2013; Fernandino et al., 2015; Hauk et al., 2004; Noppeney et al., 2006; Rabini et al., 2021; Ubaldi et al., 2022). A remaining area of uncertainty is the hierarchical and temporal organisation of the various elements of the semantic system.

Electrophysiological studies have also provided insight into the timing of semantic access processes. Semantic processing has most often been studied within the context of the n400 potential. Originally identified as the evoked response to a semantically anomalous word occurring in a sentence (*'the man went to the park to walk his tomato';* Kutas and Hillyard, 1980) subsequent work has demonstrated the wide range of contextually incongruent linguistic and non-linguistic (pictures, sounds, faces) stimuli that elicit this potential (see Kutas and Federmeier, 2011 for a review). While decades of studies of the n400 have provided invaluable insight into semantic processing, the processing underlying this component remains uncertain, and the n400 likely reflects cognitive processes extending beyond semantic processing of the concept to recalibration and reorganisation operations elicited by the

* Corresponding author.
E-mail address: scott.fairhall@unitn.it (S.L. Fairhall).

https://doi.org/10.1016/j.neuroimage.2022.119405.
Received 3 August 2021; Received in revised form 11 June 2022; Accepted 21 June 2022
Available online 22 June 2022.

unexpected nature of the oddball stimulus. More recent work employing multivariate pattern analysis (MVPA) techniques have focussed on the processing of words in non-anomalous contexts. The meaning of words, indexed as the sensitivity to semantic content (object-category), can be decoded from the emerging MEG responses as early as 200–230 msec after stimulus presentation, both when processing the names of famous people and places or words drawn from different object categories (Giari et al., 2020; Leonardelli et al., 2019). Moreover, the differences in the neural response to different semantic classes persists and is detectable until 600 msec, consistent with multiple stages of conceptual processing, potentially across multiple brain regions.

The relationship between the different regions identified in fMRI research and different temporal components identified in MEG and EEG studies remains largely unresolved. While source reconstruction provides a potential strategy to reconcile findings across electrophysiological and haemodynamic imaging modalities, source localisation remains probabilistic with accompanying statistics reflecting the reliability of the solution across participants, rather than its veracity. At the same time, haemodynamic and electrophysiological measures are most sensitive to different properties of neuronal activity (Logothetis et al., 2001; Michel et al., 2004), creating an additional challenge. One relatively novel approach to overcome some of these limitations is similarity-based fMRI-MEG fusion (Cichy et al., 2014; Cichy and Oliva, 2020). Here, the abstraction away from the neural measures themselves to the informational spaces represented in the neural response may better allow reconciliation of disparate methodologies with respect to the direct comparison of these neural measures. Representational similarity analysis (RSA) has been widely used to reconcile e findings from different measures (Kriegeskorte and Kievit, 2013). RSA works by constructing an informational space based on similarity/dissimilarity of the neural responses produced by a range of stimuli or conditions, which can then be compared to another model similarity-space. The strength of the RSA approach is in the generation of an informational space abstracted away from the original dependant measure, allowing the comparison of neural states across a broad range of measures — across behavioural and neural indices, species and neuroimaging modalities. fMRI-MEG fusion is an application of this approach that permits comparisons between MEG and fMRI, thus allowing the representations present in different brain regions to be resolved in the evolving MEG response.

The objective of the present study is to isolate representational spaces present in the MEG response over time to identify convergence with representational spaces present in regions of the fMRI-delineated semantic system. We present words drawn from 9 different semantic classes while participants performed a semantic judgments task — in both the MEG and fMRI scanners. Gaining understanding of the temporal sequence of recruitment of regions within the representational system can provide insight into the hierarchical organisation of conceptual processing. We hypothesise that regions involved in semantic control will be activated earlier and that regions involved in higher-level semantic representation will have a longer time course than regions involved in initial, automatic, conceptual representation.

1. Materials & methods

This multimodal neuroimaging study consisted of two sessions: one MEG and one fMRI. The experimental paradigm utilised in each of the two session was identical, as our goal was to perform RSA across the two neuroimaging techniques.

1.1. Participants

Twenty-three participants (12 male; mean age 25.8 years, SD = 5.4) partook in this study. All participants were right-handed native Italian speakers and reported no history of neurological disorders. One participant was excluded due to MEG artifacts produced by a metallic retainer; one did not complete the fMRI session; one subject was excluded due to excessive head movements and one subject was excluded from the MEG study but not the fMRI study due to large low frequency artifacts in the MEG recording.

Due to technical issues with the MR scanner, the order of the MEG and fMRI sessions was not fully counterbalanced. Six participants performed the fMRI session first, while 16 performed the MEG session first. As this study does not consider differences between fMRI and MEG, this does not influence the validity of the reported results. The mean time between experimental sessions was 6.7 days.

All participants gave written informed consent, and all procedures were approved by the Ethics Committee of the University of Trento.

1.2. Stimuli

Stimuli consisted of written words (in Italian; 3–10 letters) from nine semantic categories: *Body parts, Tools, Furniture, Materials & Substances, Flora, Mammals, Birds, Food, Fruits & Vegetables.* 32 exemplars were selected for each category (a total of 288 stimuli; see supplemental materials table S1 for a complete list). One-way ANOVA indicated no significant difference between categories in word length ($F<1$) nor in log word-frequency ($F<1$; Lyding et al., 2015).

1.3. Procedure

MEG and fMRI sessions employed identical experimental paradigms. Each session was composed of six runs, and each run consisted of 18 blocks of 8 stimuli from each category. Thus, each run presented two blocks of the same category. Blocks were 14 s each and were separated by a 6 s rest period (total time per run was 7.8 min). Block order was pseudo-randomised within runs so that each half of the session contained blocks for each of the nine categories. In total, 864 trials were collected: 96 for each category, and each stimulus was presented three times in the experiment.

Stimuli were presented against a grey background. Blocks were preceded by a blue fixation cross of 4 s, followed by a cue (the name of the category) for 1 s in black font, followed by a black fixation cross of 1 s. Trials consisted of a stimulus (word) presented in black for 300 msec, followed by a fixation cross which remained on the screen until the end of the trial. Trials were jittered, and the inter-trial intervals ranged randomly for 2250–2850 msec (mean: 2525 msec, uniform distribution). On each trial, participants rated the typicality of the exemplar within its semantic category (e.g., rating the typicality of “apple” or “coconut” as a fruit) on a scale from 1 (very typical) to 4 (not typical). Participants responded bimanually (two buttons for each hand).

Before both experimental sessions, participants practised a short form of the experiment (two blocks), employing stimuli not used in the main experiment.

1.4. MEG data acquisition

Electromagnetic brain activity was recorded at the centre for Mind/Brain Sciences of the University of Trento. The MEG system is composed of 306 channels (204 planar gradiometers, 102 magnetometers) from Elekta-Neuromag Ltd., Helsinki, Finland, and is placed in a magnetically shielded room (AK3B, Vakuumschmelze, Hanau, Germany). Prior to the session, the individual head shape of each participant was measured using a Polhemus FASTRAK 3D digitiser (Polhemus, Vermont, USA). The procedure involved the acquisition of three fiducial points (nasion, both preauricular sites) and the positioning of five coils (one each on the left and right mastoids, and three on the forehead). Head movements were controlled before each run of the experiment by inducing a non-invasive current through the five coils. Data was acquired with a sampling rate of 1000 Hz, and hardware filters were adjusted to bandpass the MEG signal in the frequency range of 0.01–330 Hz.

Presentation was controlled using Psychtoolbox (Brainard, 1997). Each image was back-projected with a VPixx PROPixx projector at the centre of a translucent screen placed 120 cm from the eyes of the participant. Refresh rate of the screen was 120 frames per second. Timing was verified via a photodiode.

1.5. MEG data preprocessing and analysis

Offline data was visually inspected to identify noisy channels, prior to application of the MaxMove function of the Elekta Maxfilter software (http://imaging.mrc-cbu.cam.ac.uk/meg/Maxfilter). For each subject, a reference run was identified as the one that minimised the distance in head position between runs. All other runs were realigned to this head position through the temporal signal space separation method (TSSS; Taulu & Simola, 2006) as implemented in MaxFilter software.

After maxfiltering, data was imported into Fieldtrip (Oostenveld et al., 2011) and was low-pass filtered at 70 Hz and filtered for line noise removal, then down-sampled to 200 Hz, after which, each trial's timing was corrected according to the photodiode's information. Data was then cut into epochs of 1.1 s (0.1 s pre- and 1 s post-stimulus). Trials were visually inspected to discard trials that deviated from general variance. About 5.6% of trials were removed from the analysis. All trials were baseline corrected using the baseline window (from −0.1 to 0 s), trial onsets were jittered to minimise anticipatory effects.

To consider the different measurement units of magnetometer [T] and gradiometer [T/m] sensors, the magnetometer data was multiplied by a factor of 17, corresponding to their distance in mm from the gradiometers.

1.6. fMRI data acquisition

Data were acquired at the centre for Mind/Brain Sciences, with a Prisma 3T scanner (Siemens AG, Erlangen, Germany) and using a 64-channel head coil. Visual stimuli (written words) were presented through a mirror system connected to a 42″ LCD monitor (MR-compatible, Nordic NeuroLab) positioned at the back of the magnet bore. Functional images were acquired using echo planar (EPI) T2*-weighted scans. Acquisition parameters were: repetition time (TR) of 2 s, an echo time (TE) of 28 ms, a flip angle of 75°, a field of view (FoV) of 100 mm, and a matrix size of 100×100. Total functional acquisition consisted of 1440 vol, for the six experimental runs. Each of 78 axial slices (which covered the whole brain) had a thickness of 2 mm and gap of 2 mm, AC/PC aligned. High-resolution (1 × 1 × 1 × mm) T1-weighted MPRAGE sequences were also collected (sagittal slice orientation, centric phase encoding, image matrix = 288 × 288, FoV = 288 mm, 208 slices with 1-mm thickness, TR = 2290 msec, TE = 2.74 msec, inversion time (TI) = 950 msec, 12° flip angle).

1.7. fMRI data preprocessing and analysis

Analysis was performed in SPM12 (http://www.fil.ion.ucl.ac.uk/spm/software/spm12/). The first four volumes of each run were discarded. All subsequent images were corrected for head movement. All images were normalised to the forward field obtained from segmentation, resampled to a 2 mm isotropic voxel size, and spatially smoothed using an isotropic Gaussian kernel of 5 mm FWHM.

Univariate analysis was performed at the level of each voxel. Data were high-pass filtered at 128 s and pre-whitened by means of an autoregressive model AR(1). Subject-specific beta weights were derived through a general linear model (GLM). For each subject, the data were best-fitted at every voxel using a combination of effects of interest (the nine categories). These were delta functions representing the onset of each of the experimental conditions, convolved with the SPM12 haemodynamic response function. The six motion regressors were included as variables of no interest.

2. Multivariate analysis

2.1. Within-imaging-modality classification

All multivariate analysis was performed using the CoSMoMVPA toolbox for Matlab (Oosterhof et al., 2016).

MEG data was classified using a correlation-based classifier to classify each category-pair based on the amplitude values of the 306 MEG sensors over each timepoint using a 25 msec sliding window. MEG trials were divided into 12 chunks, and classification was performed across runs using a leave-one-out cross-validation approach. To account for differing numbers of trials in each condition (following artefact rejection), a balanced number of trials was selected for each classification step, and this was repeated until each trial had been represented four times. This process was repeated 36 times for each pair-wise category comparison and the results averaged for each subject. Group-level analysis was performed using a one-sample *t*-test at each time-point after subtracting chance accuracy (0.5).

Localised patterns of information in fMRI data were obtained using the searchlight method (Kriegeskorte et al., 2006). For each subject, for each voxel v, we extracted category-specific beta patterns in a sphere centred at *v* with a radius of 4 voxels and mean centred by subtracting the mean of each voxel from each sample within that voxel (Diedrichsen and Kriegeskorte, 2017). A correlation-based classifier was used to classify each pair of categories (36 categories). Classification was performed across runs using a standard leave-one-out cross-validation approach. Resulting pair-wise classification accuracies were then averaged, yielding a single brain map for each subject. For second-level analysis, brain maps for each subject were entered into a one-sample *t*-test after subtracting chance accuracy (0.5).

2.2. MEG-fMRI integration through representational similarity analysis

Cross-modality RSA was based on the construction of 9 × 9 representational dissimilarity matrices (RDMs) containing the pairwise distance value between different categories. This was calculated for multiple spatial localisations within the fMRI data and multiple temporal windows for the MEG data.

MEG-RDM. For each subject, trials from each category were averaged and mean-centred by removing the mean within each category. At each time point, we calculated dissimilarity of pattern vectors ($1\text{-}r_{Pearsons}$) between condition pairs across the 306 sensors. To increase signal-to-noise and power, we averaged the RDMs in a time window of 50 msec, starting from 200 msec until 800 msec. Results were then averaged across subjects resulting in 12 MEG RDMs, one for each 50 msec of activity.

fMRI-RDM. Localised patterns of information were obtained using the searchlight method (Kriegeskorte et al., 2006). For each subject, for each voxel v, we extracted and mean-centred category-specific beta patterns in a sphere centred at *v* with a radius of 4 voxels. For each pair of conditions, the pairwise dissimilarity between pattern vectors was calculated ($1\text{-}r_{Pearsons}$). This procedure resulted in one fMRI-RDM for each voxel in the brain.

To relate space and time, we compared fMRI RDMs with MEG RDMs. For 50 msec time-windows, running from 200 to 800 msec post-stimulus onset, we computed the similarity between its relevant MEG-RDM and the fMRI-RDMs of each voxel. This produced a brain map of the convergence of representational similarity spaces at each time window.

2.3. Statistics

Statistical analysis of MEG MVPA was performed by first identifying timepoints where classification accuracy was significantly above chance using a one-sample *t*-test. The probability of observing temporally contiguous significant timepoints under the null hypothesis was then determined via a permutations test. Specifically, for each participant, ten null distributions were created by randomly shuffling the condition labels of

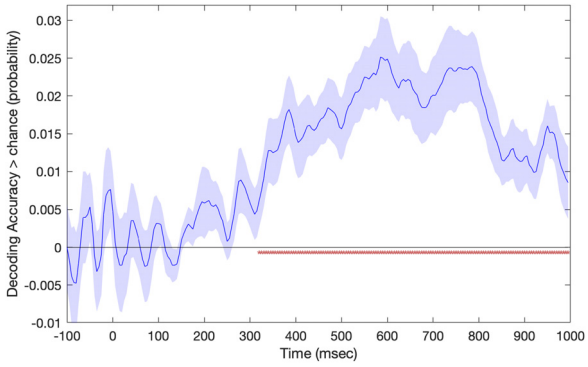

Fig. 1. Multivariate pattern classification of object-category for MEG data. Shown is the average (above chance) classification accuracy across the nine object-categories. Data were processed over a moving time window of ±20 msec. Asterisks indicate significant above-chance classification using an initial p-value of 0.05 and correcting for multiple comparisons using the extent of the temporal cluster and permutation testing.

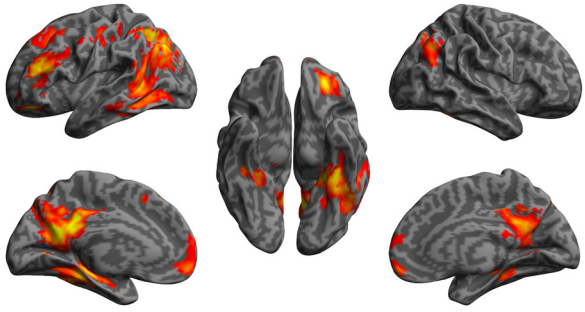

Fig. 2. Multivariate pattern classification of object-category for fMRI data. Searchlight analysis showing greater-than-chance average pair-wise classification between the nine object-categories. Initial voxel-wise threshold = $p<.001$, $p<.05$ cluster-corrected for multiple comparisons.

each block. One such null distribution was then randomly selected for each participant, a one-tailed one-sample *t*-test performed at each time-point ($p<.05$), and the largest temporal cluster in each permutation was identified. This was repeated 10,000 times to determine the probability under the null of a temporal cluster of a given size across the whole time-window of interest (200–800 msec). The reported temporal cluster in Fig. 1 exceeded this extent-threshold.

Statistical analysis of fMRI MVPA utilised an initial voxel-wise threshold of $p<.001$ and corrected for multiple comparisons at the cluster level via random field theory (Worsley et al., 1996).

MEG-informed RSA of fMRI data involved corrections both over voxels and over time windows. Contiguous clustering in this context can occur both over space and time. Corrections for multiple comparisons utilised an initial voxel-wise $p<.001$ and 100-voxel extent threshold and multiple-comparison correction determined by the extent of spatiotemporal clusters. For each participant, 20 null distribution MEG RSAs were created in an identical manner to the veridical analysis, except that the block category labels were randomly mislabelled. One such mislabelled time-series was randomly selected for each participant, the MEG-fMRI RSA was performed for each participant, and a group-level GLM performed. This process was repeated 1000 times, and the maximum contiguous cluster across space and time for each permutation computed, which allowed determination of the probability of a cluster in the veridical analysis exceeding this space-time extent threshold under the null hypothesis.

3. Results

3.1. Behavioural

Reaction Times (RTs) did not significantly differ as a function of modality (MEG/fMRI), nor was there an interaction between imaging modality and category (F-values<1). RTs did show a main effect of category $F_{(3.02,57.30)}=8.90$, $p<.001$, Greenhouse-Geisser corrected. The fastest responses were made for food items (mean = 937 msec) and the slowest responses for tool items (mean = 1019 msec). Mean reaction times for each category and imaging modality are provided in supplemental materials, table S2.

3.2. Category classification - MEG

We initially considered each neuroimaging modality separately and investigated if it is possible to discriminate semantic categories. The average overall classification performance (collapsed across category pairs) for MEG data is shown in Fig. 1. An initial temporal cluster spanning from 275 to 295 msec did not survive correction for multiple comparison. This was followed by an extended temporal cluster spanning from 320 msec to the end of the analysed time window ($p\leq.0001$, corrected).

3.3. Category classification – fMRI

For fMRI, the average overall classification performance (collapsed across category pairs) is shown in Fig. 2. It revealed sensitivity to semantic category in the AG, precuneus/posterior cingulate, orbitofrontal cortex (OFC), IFG, superior frontal sulcus (SFG), posterior middle/inferior temporal gyrus (pMTG/ITG), ventral temporal cortex (VTC; comprising fusiform, parahippocampal, and perirhinal cortex), as detailed in Table 1.

3.4. MEG-fMRI integration through representational similarity analysis

We used RSA to compare neural representational similarity between MEG and fMRI. Fig. 3 shows clusters corrected for multiple comparisons across the volume. Table 2 indicates which clusters survived multiple-comparison correction both across the volume and the 12 time-windows.

Representational spaces align between MEG and fMRI firstly in the 350–395 time-window, where object-category representation present in the MEG converge with representational spaces in the pITG. The pITG cluster persisted in the 400–445 time window, creating a contiguous spatiotemporal cluster that survived corrections for multiple comparisons across both the volume and number of time windows ($p=.025$, corrected). In the 400–445 time window, the pITG cluster was observed

Table 1
Significance, extent and location of multivariate pattern classification accuracy of object-category for fMRI data. For large clusters, local maxima (>20 mm apart) are listed separately.

	cluster		peak			
	$P_{(FWE-corr)}$	voxels	T	*x*	*y*	*z*
left AG	<0.001	14,572	10.09	−36	−70	42
precuneus			8.53	−8	−58	22
left VTC			7.62	−38	−32	−22
left OFC	<0.001	14,572	8.16	−26	−40	−12
vmPFC			6.42	−2	54	−10
left IFG	<0.001	2011	7.97	−38	36	16
left SFS			6.16	−12	20	40
right VTC	0.021	464	6.01	28	−34	−16
right AG	<0.001	1226	5.93	40	−62	36

Abbreviations. AG: angular gyrus; VTC: ventrotemporal cortex; OFC: orbitofrontal cortex; vmPFC: ventromedial PFC; IFG: inferior frontal gyrus; SFS: superior frontal sulcus.

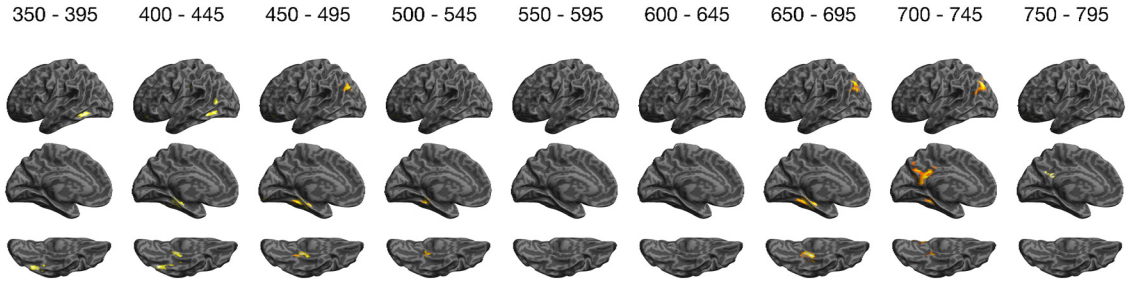

Fig. 3. Whole-brain MEG-fMRI RSA searchlight analysis. Shown are the locations of localised patterns of category representation that conform to the MEG representational space at each time window. Significant voxels are shown with an initial voxel-wise threshold of $p<.001$, which survived cluster-extent corrections for multiple comparisons across both the brain volume and time windows. See table 2 cluster location and extent. No significant clusters were evident in the time windows between 200 and 345 msec.

Table 2
Cluster peak coordinates and number of voxels for the whole brain MEG-fMRI RSA searchlight analysis shown in figure 3. Contiguous temporal clusters are indicated with grey shading and survived corrections for multiple comparisons over both the brain volume and the 12 time-windows.

Time Window									
Region	350–395	400–445	450–495	500–545	550–595	600–645	650–695	700–745	750–795
VTC		−32 −24 −22 [201]	−26 −36 −16 [286]	−28 −36 −16 [100]			−26 −36 −14 [441]	−28 −38 −14 [105]	
pITG	−52 −56 −12 [254]	−48 −62 −8 [283]							
AG							−32 −74 34 [557]	−32 −76 40 [856]	
Precuneus								−8 −46 24 [768]	6 −46 30 [130]

Abbreviations. VTC: ventrotemporal cortex; pITG: posterior inferior temporal gyrus; AG: angular gyrus; IFG: inferior frontal gyrus; OFC: orbitofrontal cortex; pSTS: posterior superior temporal sulcus; MFG: middle frontal gyrus.

to be accompanied by MEG/fMRI representational convergence in the VTC, which formed a congruous spatial temporal cluster that extended to the 500–545 msec time window (p=.019, corrected). Subsequent MEG/fMRI representational convergence was observed after 650 msec: again in the VTC, from 650 to 745 msec (p=.021, corrected), in the left angular gyrus from 650 to 745 msec ($p \leq .001$, corrected) and in the precuneus from 700 to 795 msec (p=.004, corrected).

4. Discussion

In this work, we used similarity-based fMRI-MEG fusion to gain insight into the temporal properties of components of the brain's semantic system. Within-imaging-modality-classification analysis revealed sensitivity to semantic object-category emerging around 320 msec post-stimulus in the MEG data, while fMRI data indicated widespread sensitivity to object-category across multiple brain regions associated with the semantic system. Similarity-based fMRI-MEG fusion indicated multi-phase processing across elements of the semantic system. Positive evidence for convergent semantic spaces between MEG and fMRI emerged first in left pITG and VTC around 350–450 msec after stimulus onset. This was followed by shared MEG/fMRI representational spaces after 650 msec that extended beyond VTC to incorporate the precuneus and the left angular gyrus. Broadly, this is consistent with early involvement of a subset of regions associated with conceptual representation, followed by more widespread representation across the semantic system, incorporating elements within the default mode network.

4.1. Early representational system – 350–545 msec

Representational spaces converged between localised spatial patterns in the pITG and VTC and the MEG trace in the 350–545 msec time period. Sections of the pITG corresponding to the peak of the present study have been shown not only to contain cross-modal (word/picture) representations of semantic object-categories but convergence between the neural and semantic distances between categories (S.L. Fairhall and Caramazza, 2013), providing stringent evidence for the representation of conceptual knowledge in this region. While pITG and VTC regions are more posterior than the anterior aspect of ventral temporal cortex most strongly associated with semantic dementia, a form of primary progressive aphasia that leads to deficits in semantic knowledge, neural degeneration associated with semantic dementia also encompasses both the pITG and VTC (Hodges et al., 1992; Rosen et al., 2002). These regions may be functionally associated with those more anterior temporal regions that have long been implicated as part of a multimodal hub linking together conceptual knowledge distributed across the cortex (Lambon-Ralph et al., 2017; Patterson et al., 2007).

It is notable that of the distributed set of regions showing multivariate sensitivity to object-category during semantic typicality judgments, it is only in regions corresponding to the VTC and pITG that contain categorical representational patterns that are also present when semantic access is incidental (i.e. when participants perform a phonetic judgement on the word stimulus (Liuzzi et al., 2021). The automatic nature of representational access in these regions is consistent with the primacy of representational fMRI/MEG convergence in these regions in the present study. Collectively, these results suggest that automatic and relatively early semantic representation may occur within left VTC and pITG, potentially providing a first draft of the semantic information that is contained in the stimulus that is further elaborated at subsequent stages to allow performance of the typicality task.

The pITG cluster extends into the pMTG, a region implicated in semantic control operations (Jackson, 2021; Lambon-Ralph et al., 2017). While pMTG is more active during tasks that require making weak, infrequent, semantic associations (Davey et al., 2016), and TMS to pMTG interferes with performance on such demanding semantic tasks (Whitney et al., 2011), this region responds selectively for specific semantic classes such as 'tools' (Chao et al., 1999; Noppeney et al., 2006),

shows sensitivity to other object categories when tools are not included in the category set (S L Fairhall and Caramazza, 2013) and it is uncertain whether this activation reflects representational or control processes in the present study.

4.2. Late representational system – 650–800 msec

In the 650 to 800 msec time period, convergence between fMRI and MEG representational spaces was present not only in VTC but extended to the left angular gyrus, precuneus. The angular gyrus and precuneus are key components of the default mode network and are implicated in a range of higher-order internalised cognition extending beyond semantic processing to include theory of mind, remembering the past and imagining the future (Buckner and DiNicola, 2019; Spreng et al., 2009). Within the context of the current task, these regions may play a role in elaborating upon representations accessed in pITG and VTC to facilitate the semantic typicality judgement of the exemplar within its category. This is consistent with the role of the angular gyrus in thematic links between object-concepts (mouse, cheese; Schwartz et al., 2011) and the role of the precuneus in linking together concepts drawn from different object domains when presented in sentences (Rabini et al., 2021). Moreover, the time course of activation in the precuneus is also consistent with fMRI indices of the rapidity with which information can be extracted about famous individuals from the rapid serial presentation of their faces (Ubaldi and Fairhall, 2021).

These results should be considered within the context of the current experimental paradigm. This typicality task required lexical access to the word stimuli, retrieval of the associated conceptual representation and comparison of the exemplar to the category in general to allow typicality assessment. Due to the arbitrary and symbolic nature of alphabetic languages, it is unlikely that lexical access would differ as a function of semantic category. In this way, the first sensitivity to semantic class, that occurring between 350 and 545 msec, may reflect the automatic retrieval of the semantic representation associated with word presentation to skilled reading and would generalise across experiments employing word stimuli. On the other hand, if the further elaboration of conceptual representations necessary for the typicality judgement is driving later components in the precuneus and left angular gyrus, this aspect of the results may not generalise to tasks that do not share such demands. Additionally, the precise time course of representational activation may be influenced by the paradigm. Specifically, the predictability of the semantic category of the upcoming stimuli within each blocked and the repetition of stimuli (at total of 3 times over the entire experiment) may have facilitated stimulus processing, resulting in relatively shorter access latencies compared to other experimental paradigms.

While these results provide broad insight into earlier and later stages of conceptual representation, this likely represents only a partial picture of the temporal properties of conceptual access. With the potential exception of the pMTG, the current results are blind to the time course of semantic control processes such as those taking place in the IFG, which shows sensitivity to semantic category in the fMRI MVPA analysis (Fig. 2) and is known to be recruited when semantic judgements are known to be required (Zhang et al., 2021). One clear possibility is that MEG fMRI convergence is present in this region in the investigate time-period but is below the resolution of the current study. Likewise, more subtle shared representational spaces may be present at time points earlier than the 350 msec, where previous MEG work has shown sensitivity to semantic content (Giari et al., 2020; Leonardelli et al., 2019) as have chronometric TMS studies (Teige et al., 2018), as well as at other cortical sites and time periods.

In this work, we employed RSA to align neural representational spaces between MEG and fMRI to gain insight into the temporal processing hierarchy of the brain's semantic system. Consistent with a role in automatic processing, we saw the MEG and fMRI representational spaces aligned first in the pITG and VTC around the 350–450 msec time window. This was followed by later representational convergence after 650 msec that extended to the precuneus and angular gyrus, default mode regions broadly associated with internalised cognitive processes weakly associated with cognition involving interaction with the environment. Collectively, these results are consistent with a multistage conceptual processing of word stimuli, initially involving automatic aspects of the representational system and later extending to elements of the semantic system more strongly associated with internalised cognitive states.

Credit authorship contribution statement

Elisa Leonardelli: Formal analysis, Investigation. **Scott L. Fairhall:** Conceptualization, Formal analysis, Writing - original draft, Funding acquisition, Supervision.

Data availability statement

Thresholds t-statistic maps for within modality fMRI category decoding and MEG-fMRI analysis for each time window are freely available on the Open Science Framework (OSF) at the following URL: https://osf.io/8qfw4/?view_only=3d50679935434bdf84a582ad7db96231.

Declaration of Competing Interest

The authors declare that they have no known competing financial interests or personal relationships that could have appeared to influence the work reported in this paper.

Acknowledgements

The project was funded by the European Research Council (ERC) grant CRASK – Cortical Representation of Abstract Semantic Knowledge, awarded to Scott Fairhall under the European Union's Horizon 2020 research and innovation program (grant agreement no. 640594). MRI scanning is supported by funding from the Caritro Foundation, Italy.

Supplementary materials

Supplementary material associated with this article can be found, in the online version, at doi:10.1016/j.neuroimage.2022.119405.

References

Badre, D., Poldrack, R.A., Paré-Blagoev, E.J., Insler, R.Z., Wagner, A.D., 2005. Dissociable controlled retrieval and generalized selection mechanisms in ventrolateral prefrontal cortex. Neuron 47, 907–918. doi:10.1016/j.neuron.2005.07.023.

Binder, J.R., Desai, R.H., Graves, W.W., Conant, L.L., 2009. Where Is the Semantic System? A Critical Review and Meta-Analysis of 120 Functional Neuroimaging Studies. Cereb. Cortex 19, 2767–2796. doi:10.1093/cercor/bhp055.

Brainard, D.H., 1997. The Psychophysics Toolbox. Spatial Vision 10 (4), 433–436.

Bruffaerts, R., Dupont, P., Peeters, R., De Deyne, S., Storms, G., Vandenberghe, R., 2013. Similarity of fMRI activity patterns in left perirhinal cortex reflects semantic similarity between words. J. Neurosci. 33, 18597–18607. doi:10.1523/JNEUROSCI.1548-13.2013.

Buckner, R.L., Andrews-Hanna, J.R., Schacter, D.L., 2008. The brain's default network: anatomy, function, and relevance to disease. Ann. N. Y. Acad. Sci. doi:10.1196/annals.1440.011.

Buckner, R.L., DiNicola, L.M., 2019. The brain's default network: updated anatomy, physiology and evolving insights. Nat. Rev. Neurosci. doi:10.1038/s41583-019-0212-7.

Chao, L.L., Haxby, J.V., Martin, A., 1999. Attribute-based neural substrates in temporal cortex for perceiving and knowing about objects. Nat. Neurosci. doi:10.1038/13217.

Cichy, R.M., Oliva, A., 2020. A M/EEG-fMRI Fusion Primer: resolving Human Brain Responses in Space and Time. Neuron doi:10.1016/j.neuron.2020.07.001.

Cichy, R.M., Pantazis, D., Oliva, A., 2014. Resolving human object recognition in space and time. Nat. Neurosci. 17, 455–462. doi:10.1038/nn.3635.

Davey, J., Thompson, H.E., Hallam, G., Karapanagiotidis, T., Murphy, C., De Caso, I., Krieger-Redwood, K., Bernhardt, B.C., Smallwood, J., Jefferies, E., 2016. Exploring the role of the posterior middle temporal gyrus in semantic cognition: integration of anterior temporal lobe with executive processes. Neuroimage 137, 165–177. doi:10.1016/j.neuroimage.2016.05.051.

Devereux, B.J., Clarke, A., Marouchos, A., Tyler, L.K., 2013. Representational Similarity Analysis Reveals Commonalities and Differences in the Semantic Processing of Words and Objects. J. Neurosci. 33, 18906–18916. doi:10.1523/JNEUROSCI.3809-13.2013.

Diedrichsen, J., Kriegeskorte, N., 2017. Representational models: a common framework for understanding encoding, pattern-component, and representational-similarity analysis. PLoS Comput. Biol. 13, 1–35. doi:10.1371/journal.pcbi.1005508.
Fairhall, S.L., 2020. Cross recruitment of domain-selective cortical representations enables flexible semantic knowledge. J. Neurosci. doi:10.1523/JNEUROSCI.2224-19.2020, JN-RM-2224-19.
Fairhall, S.L., Anzellotti, S., Ubaldi, S., Caramazza, A., 2014. Person- and place-selective neural substrates for entity-specific semantic access. Cereb. Cortex 24, 1687–1696. doi:10.1093/cercor/bht039.
Fairhall, S.L., Caramazza, A., 2013a. Brain regions that represent amodal conceptual knowledge. J. Neurosci. 33. doi:10.1523/JNEUROSCI.0051-13.2013.
Fairhall, S.L., Caramazza, A., 2013b. Category-selective neural substrates for person- and place-related concepts. Cortex 49, 2748–2757. doi:10.1016/j.cortex.2013.05.010.
Fernandino, L., Binder, J.R., Desai, R.H., Pendl, S.L., Humphries, C.J., Gross, W.L., Conant, L.L., Seidenberg, M.S., 2015. Concept representation reflects multimodal abstraction: a framework for embodied semantics. Cereb. Cortex 1–17. doi:10.1093/cercor/bhv020.
Giari, G., Leonardelli, E., Tao, Y., Machado, M., Fairhall, S.L., 2020. Spatiotemporal properties of the neural representation of conceptual content for words and pictures – an MEG study. Neuroimage doi:10.1016/j.neuroimage.2020.116913.
Hauk, O., Johnsrude, I., Pulvermüller, F., 2004. Somatotopic Representation of Action Words in Human Motor and Premotor Cortex. Neuron 41, 301–307. doi:10.1016/S0896-6273(03)00838-9.
Hodges, J.R., Patterson, K., Oxbury, S., Funnell, E., 1992. Semantic dementia: progressive fluent aphasia with temporal lobe atrophy. Brain 115, 1783–1806. doi:10.1093/brain/115.6.1783.
Jackson, R.L., 2021. The neural correlates of semantic control revisited. Neuroimage doi:10.1016/j.neuroimage.2020.117444.
Kriegeskorte, N., Goebel, R., Bandettini, P., 2006. Information-based functional brain mapping. Proc. Natl. Acad. Sci. U. S. A. 103, 3863–3868. doi:10.1073/pnas.0600244103.
Kriegeskorte, N., Kievit, R.A., 2013. Representational geometry: integrating cognition, computation, and the brain. Trends Cogn. Sci. 17, 401–412. doi:10.1016/j.tics.2013.06.007.
Kutas, M., Federmeier, K.D., 2011. Thirty years and counting: finding meaning in the N400 component of the event-related brain potential (ERP). Annu. Rev. Psychol. doi:10.1146/annurev.psych.093008.131123.
Lambon-Ralph, M.A., Jefferies, E., Patterson, K., Rogers, T.T., 2017. The neural and computational bases of semantic cognition. Nat. Rev. Neurosci. 18, 42–55. doi:10.1038/nrn.2016.150.
Leonardelli, E., Fait, E., Fairhall, S.L., 2019. Temporal dynamics of access to amodal representations of category-level conceptual information. Sci. Rep. 9. doi:10.1038/s41598-018-37429-2.
Liuzzi, A.G., Aglinskas, A., Fairhall, S.L., 2020. General and feature-based semantic representations in the semantic network. Sci. Rep. doi:10.1038/s41598-020-65906-0.
Liuzzi, A.G., Bruffaerts, R., Dupont, P., Adamczuk, K., Peeters, R., De Deyne, S., Storms, G., Vandenberghe, R., 2015. Left perirhinal cortex codes for similarity in meaning between written words: comparison with auditory word input. Neuropsychologia 76, 4–16. doi:10.1016/j.neuropsychologia.2015.03.016.
Liuzzi, A.G., Ubaldi, S., Faiirhall, S.L., 2021. Representations of conceptual information during automatic and active semantic access. Neuropsychologia 160, 107953. doi:10.1016/j.neuropsychologia.2021.107953.
Logothetis, N.K., Pauls, J., Augath, M., Trinath, T., Oeltermann, A., 2001. Neurophysiological investigation of the basis of the fMRI signal. Nature doi:10.1038/35084005.
Lyding, V., Stemle, E., Borghetti, C., Brunello, M., Castagnoli, S., Dell'Orletta, F., Dittmann, H., Lenci, A., Pirrelli, V., 2015. The PAISÀ Corpus of Italian Web Texts 36–43. https://doi.org/10.3115/v1/w14-0406
Martin, A., Chao, L.L., 2001. Semantic memory and the brain: structure and processes. Curr. Opin. Neurobiol. doi:10.1016/S0959-4388(00)00196-3.
Michel, C.M., Murray, M.M., Lantz, G., Gonzalez, S., Spinelli, L., Grave De Peralta, R., 2004. EEG source imaging. Clin. Neurophysiol. doi:10.1016/j.clinph.2004.06.001.
Noppeney, U., Price, C.J., Penny, W.D., Friston, K.J., 2006. Two distinct neural mechanisms for category-selective responses. Cereb. Cortex 16, 437–445. doi:10.1093/cercor/bhi123.
Oostenveld, R., Fries, P., Maris, E., Schoffelen, J.M., 2011. FieldTrip: Open Source Software for Advanced Analysis of MEG, EEG, and Invasive Electrophysiological Data. Computational intelligence and neuroscience.
Oosterhof, N.N., Connolly, A.C., Haxby, J.V., 2016. CoSMoMVPA: multi-modal multivariate pattern analysis of neuroimaging data in matlab/GNU octave. Front. Neuroinform. doi:10.3389/fninf.2016.00027.
Patterson, K., Nestor, P.J., Rogers, T.T., 2007. Where do you know what you know? The representation of semantic knowledge in the human brain. Nat. Rev. Neurosci. 8, 976–987. doi:10.1038/nrn2277.
Rabini, G., Ubaldi, S., Fairhall, S.L., 2021. Combining Concepts Across Categorical Domains: a Linking Role of the Precuneus. Neurobiol. Lang. 2, 354–371. doi:10.1162/nol_a_00039.
Rosen, H.J., Gorno-Tempini, M.L., Goldman, W.P., Perry, R.J., Schuff, N., Weiner, M., Feiwell, R., Kramer, J.H., Miller, B.L., 2002. Patterns of brain atrophy in frontotemporal dementia and semantic dementia. Neurology 58, 198–208. doi:10.1212/WNL.58.2.198.
Schwartz, M.F., Kimberg, D.Y., Walker, G.M., Brecher, A., Faseyitan, O.K., Dell, G.S., Mirman, D., Coslett, H.B., 2011. Neuroanatomical dissociation for taxonomic and thematic knowledge in the human brain. Proc. Natl. Acad. Sci. U. S. A. 108, 8520–8524. doi:10.1073/pnas.1014935108.
Simanova, I., Hagoort, P., Oostenveld, R., Van Gerven, M.A.J., 2014. Modality-independent decoding of semantic information from the human brain. Cereb. Cortex. doi:10.1093/cercor/bhs324.
Spreng, R.N., Mar, R.A., Kim, A.S.N., 2009. The common neural basis of autobiographical memory, prospection, navigation, theory of mind, and the default mode: a quantitative meta-analysis. J. Cogn. Neurosci. 21, 489–510. doi:10.1162/jocn.2008.21029.
Teige, C., Mollo, G., Millman, R., Savill, N., Smallwood, J., Cornelissen, P.L., Jefferies, E., 2018. Dynamic semantic cognition: characterising coherent and controlled conceptual retrieval through time using magnetoencephalography and chronometric transcranial magnetic stimulation. Cortex 103, 329–349. doi:10.1016/j.cortex.2018.03.024.
Thompson-Schill, S.L., D'Esposito, M., Aguirre, G.K., Farah, M.J., 1997. Role of left inferior prefrontal cortex in retrieval of semantic knowledge: a reevaluation. Proc. Natl. Acad. Sci. U. S. A. doi:10.1073/pnas.94.26.14792.
Tyler, L.K., Moss, H.E., 2001. Towards a distributed account of conceptual knowledge. Trends Cogn. Sci. 5, 244–252. doi:10.1016/S1364-6613(00)01651-X.
Ubaldi, S., Fairhall, S.L., 2021. fMRI-Indexed neural temporal tuning reveals the hierarchical organsiation of the face and person selective network. Neuroimage 227, 117690. doi:10.1016/j.neuroimage.2020.117690.
Ubaldi, S., Rabin, G., Fairhall, S.L., 2022. Recruitment of control and representational components of the semantic system during successful and unsuccessful access to complex factual knowledge. J. Neurosci. doi:10.1523/JNEUROSCI.2485-21.2022.
Wagner, A.D., Paré-Blagoev, E.J., Clark, J., Poldrack, R.A., 2001. Recovering meaning: left prefrontal cortex guides controlled semantic retrieval. Neuron doi:10.1016/S0896-6273(01)00359-2.
Whitney, C., Kirk, M., O'Sullivan, J., Lambon Ralph, M.A., Jefferies, E., 2011. The neural organization of semantic control: TMS evidence for a distributed network in left inferior frontal and posterior middle temporal gyrus. Cereb. Cortex 21, 1066–1075. doi:10.1093/cercor/bhq180.
Worsley, K.J., Marrett, S., Neelin, P., Vandal, A.C., Friston, K.J., Evans, A.C., 1996. A unified statistical approach for determining significant signals in images of cerebral activation. Hum. Brain Mapp. 4, 58–73 doi:10.1002/(SICI)1097-0193(1996)4:1<58::AID-HBM4>3.0.CO;2-O.
Zhang, M., Varga, D., Wang, X., Krieger-Redwood, K., Gouws, A., Smallwood, J., Jefferies, E., 2021. Knowing what you need to know in advance: the neural processes underpinning flexible semantic retrieval of thematic and taxonomic relations. Neuroimage 224, 117405. doi:10.1016/j.neuroimage.2020.117405.